ACTA IMEKO
ISSN: 2221-870X
September 2024, Volume 13, Number 3, 1 - 8

Experimental characterization of a novel combined composite reinforced mortar - fibre Bragg grating technology for the retrofit and control of existing structures

Stefano De Santis[1], Giovanni Moretti[1], Michele Arturo Caponero[2], Sara Fares[1], Cristina Mazzotta[2], Diego Dell'Erba[3]

[1] *Roma Tre University, Department of Civil, Computer and Aeronautical Engineering, Via Vito Volterra 62, Rome, Italy*
[2] *ENEA, Frascati Research Centre, Via Enrico Fermi 45, Frascati (RM), Italy*
[3] *Ingegneria Integrata srl, Via delle Ciliegie 141/B, Rome, Italy*

ABSTRACT
This article investigates the potential of a novel integrated system for the strengthening and monitoring of existing structures. The proposed technology combines Composite Reinforced Mortar (CRM) reinforcements and Fibre Bragg Grating (FBG) sensors and is named as CRM-FBG. Direct tensile tests were conducted as the first step of prototype development and were aimed at evaluating the performance and feasibility of the CRM-FBG system. Measurements provided by FBG sensors were compared to Digital Image Correlation data. The outcomes of the laboratory experiments showed the reliability of the proposed technology, with interesting prospective applications for the retrofit and structural health monitoring of the built heritage.

Section: RESEARCH PAPER

Keywords: retrofitting of architectural heritage; composite reinforced mortar; fiber Bragg grating sensor; digital image correlation; structural health monitoring

Citation: S. De Santis, G. Moretti, M. A. Caponero, S. Fares, C. Mazzotta, D. Dell'Erba, Experimental characterization of a novel combined composite reinforced mortar - fibre Bragg grating technology for the retrofit and control of existing structures, Acta IMEKO, vol. 13 (2024) no. 3, pp. 1-8. DOI: 10.21014/actaimeko.v13i3.1801

Section Editor: Fabio Leccese, Università Degli Studi Roma Tre, Rome, Italy

Received February 26, 2024; **In final form** July 17, 2024; **Published** September 2024

Funding: This work was supported by Regione Lazio (G03269/2022) and by Indagini Strutturali Srl (Rome, Italy).

Corresponding author: Giovanni Moretti, e-mail: giovanni.moretti2@uniroma3.it

1. INTRODUCTION

Preserving the integrity of the built heritage necessitates sustainable approaches to structural retrofitting, that ensure the long-term effectiveness of strengthening systems and continuous monitoring to detect deterioration. Among the innovative technologies for upgrading historic structures, Composite Reinforced Mortar (CRM) [1], [2] and Fabric Reinforced Cementitious Matrix (FRCM) [3]-[10] have proven particularly advantageous.

These systems involve high-strength fabrics or Fibre Reinforced Polymer (FRP) meshes, composed of carbon, glass, basalt, or aramid fibres or ultra-high tensile strength steel cords, bonded to structural elements using inorganic matrices like lime, cement, or geopolymer mortars. In recent years, the mechanical properties of FRCM and CRM composites have been deeply investigated [6]-[8] and specific design criteria have been developed [10], [11], leading to the publication of design guidelines [12], [13] and promoting field applications.

Inorganic matrix composites ensure significant enhancement of structural capacity thanks to their high strength-to-weight ratio and physical-chemical compatibility with original substrates [11]. On the other hand, there is still a critical gap in knowledge regarding their long-term behaviour. At present stage, the environmental durability of constituent materials is investigated through laboratory tests conducted after accelerated artificial aging [7], [14], as recommended by acceptance protocols [15], [16]. But, when applied in situ, the durability of FRCM/CRM reinforcements may be remarkably compromised by material degradation, cracking of the mortar matrix, and detachments with the substrate [17]-[21]. Nonetheless, current design guidelines lack clear information on monitoring and control [22]-

[24], and existing practices often rely on routine test methods for concrete or avoid testing altogether.

To address this knowledge gap, there is a pressing need to develop methodologies for assessing the condition of FRCM/CRM systems and the overall behaviour of strengthened structures during their service life. Reliable non-destructive test methods (NDTs) could offer a solution, especially for periodic inspections, and the integration of smart strengthening systems could enable continuous monitoring. In this framework, the use of optical fibres housing Fibre Bragg Grating (FBG) sensors [25] emerges as a promising avenue, though limited attempts have been made to combine them with FRCM, and no efforts at all have been directed towards CRM to date.

The proposed CRM-FBG system is envisioned to provide insights for planning and prioritizing rehabilitation works before severe damage occurs. The position of the sensor, placed on the reinforcement fabric/mesh and embedded within the matrix, could provide information on the strain and stress state, which would be unavailable using traditional technologies.

The present experimental work, led by a collaborative research group including Roma Tre University, ENEA, and Ingegneria Integrata srl, is focused on prototype development, scientific validation in the laboratory, and prospective field pilot applications. The results presented in this paper encompass direct tensile tests on Glass Fibre Reinforced Polymer (GFRP) mesh wires equipped with FBG sensors housed in optical fibres. Validation against Digital Image Correlation data underscored the reliability of the proposed CRM-FBG integrated system for combined strengthening and Structural Health Monitoring (SHM) purposes, with many potential applications ranging from architectural heritage [26] to infrastructures [27] that require continuous cost-efficient and low-impact control.

Section 2 presents the state of the art in the use of FBG sensors in civil engineering. Section 3 describes the materials used for the test. Section 4 presents the test setup and all the instrumentation used during the test. Section 5 compares the deformations recorded by the FBG sensors and those obtained from the DIC. Finally, in Section 6, the conclusions emerging from the experimental results are presented.

2. STATE OF THE ART

FBG refers to a periodic or quasi-periodic modulation of the refractive index along a short segment (typical length is 10 mm) of the core of an optical fibre. The modulation produces a diffraction grating, which operates as a wavelength-selective mirror. It reflects a narrow spectral band centred around a specific wavelength value, named Bragg wavelength (λ_B), given by Equation (1) [28]:

$$\lambda_B = 2\, n_{eff}\, \Lambda\,, \tag{1}$$

where n_{eff} represents the effective refractive index of the core at the grating and Λ the period of the refractive index modulation. Any alterations in strain or temperature occurring at the grating cause changes in both n_{eff} and Λ, resulting in a shift of λ_B, allowing to use FBGs for sensing, decoding the measure by spectroscopic analysis of the reflected light. To use FBGs as sensors, the basic technology consists in launching light with a wide spectral band into the fibre and analysing the reflected light. For sensing purposes, FBGs have shown significant promise and have seen extensive use as sensors in recent decades [29].

If no alteration in temperature occurs, the variation in strain ε_{FBG} at the FBG is given by equation (2) [28]:

$$\varepsilon_{FBG} = \frac{\Delta\lambda_B}{0.78\,\lambda_B} \tag{2}$$

where $\Delta\lambda_B$ is the central wavelength change caused by the deformation of the FBG sensor, and $0.78 = 1-C$, $C = 0.22$ being the stress-optic constant of the optical fibre [28]. Equation (2) holds in this study, since no relevant temperature perturbation occurred during test execution, and shows that the strain sensitivity of standard FBGs, which operate in the 1500÷1600 nm range, is about 1.2 pm/mε.

The FBG sensors, well-established in aerospace, automotive, biomedicine, mechanics, and industry [30], have witnessed a recent surge in applications within civil engineering, particularly for Structural Health Monitoring (SHM). In the realm of geotechnics, early applications focused on measuring accelerations and pressures for oil exploration [31], recording soil deformations and slopes, controlling foundation piles [32], and monitoring tunnel structural stability [33]. In hydraulic engineering, FBGs were employed to measure circumferential strains in pipelines [34] and for SHM of subsea structures [35]. Finally, recent studies were devoted to the integration of FBGs in polymeric 3D printed elements [36].

As regards structural engineering, FBG sensors have demonstrated effectiveness in bridge monitoring, with applications ranging from measuring strains in post-tensioned railway bridges [37] to monitoring vibrations of railway sleepers under rail traffic [38]. Verstrynge et al. [39] pioneered an integrated technique for crack monitoring in masonry structures, incorporating FBGs, Acoustic Emission sensors, and Digital Image Correlation. Antunes et al. [40] applied FBG sensors to an adobe masonry wall for detecting crack propagation (as displacement transducers) and dynamic identification (as accelerometers). The possibility of using FBG as vibration sensors for dynamic monitoring of structures has been investigated also by [41], [42], further extending the potential of this technology for the SHM of the built heritage.

The integration of FBG sensors into technical textiles, widely applied in the structural retrofit and seismic upgrade of earthen-work and masonry structures, emerges as a promising solution. Over the past 15 years, the incorporation of FBG sensors for monitoring within technical textiles possessing reinforcing capabilities has been a focal point [43]. Liehr et al. [44] detailed initiatives under the EU project POLYTECT [45], highlighting the development of innovative geotextiles embedded with FBGs for monitoring geotechnical and masonry structures. Smart textiles showcased cost-effectiveness in reinforcing and monitoring structures, enhancing ductility, and providing damage alerts [44].

Valvona et al. [46] demonstrated the efficacy of seismic retrofitting and monitoring integrated systems, combining glass fabric reinforced cement mortar (GFRCM) composites with FBG sensors to monitor strengthened masonry structures. Placing FBG sensors strategically near expected cracks and debonding sites, the authors successfully decoupled mechanical and thermic strains, allowing for the detection of strains due to temperature variation and isolation of those generated by loads.

Shaikh et al. [47] explored the use of discrete FBGs and Brillouin optical time domain reflectometry (BOTDR) in concrete beams reinforced with different FRCM systems. Measurements from these optical sensors were compared with those from traditional strain gauges, revealing valuable insights into their performance and potential applications.

Coricciati et al. [48] introduced smart FRP devices embedding FBG sensors and Distributed Fiber Optic Sensors (DFOS) to reinforce and monitor masonry structures effectively. Tetta [49] investigated the use of FBG sensors integrated with FRCM composites, revealing promising prospects for monitoring externally applied FRCM jacketing on existing structures.

Saidi and Gabor [50] analysed the tensile behaviour of FRCM composites with DFOS, shedding light on matrix and interface responses. Stempniewski et al. [51] reported findings from the POLYMAST project, employing composite seismic wallpaper with embedded FBG sensors for structural health monitoring. Finally, Bertolesi et al. [22] explored bond slip behaviour in strengthening materials using DFOS strain sensors.

These endeavours reflect the applications and continual evolution of FBG sensors in structural monitoring contexts. The feasibility of the use of FBGs for strain monitoring of FRP materials, also in the prospective of in-field applications in civil engineering, is well assessed as per many of the above recalled references. The use of FBGs in mortar-based components is reported by Lima et al. [52]. Huafu and coworkers [53] pointed out the practical advantages of using FBGs instead of conventional electric sensors. The choice of FBG sensors for this study was specifically addressed by the low intrusiveness of both the cabling and the sensing component, which ensure that the proper embedding of the FRP mesh in the matrix is not compromised. Many FBGs can stay cabled in series along a single optical fibre, which can be effectively protected for safe manipulation in standard tight tubing for telecom applications, whose diameter is so small as 0.9 mm. The signal of all FBGs is delivered along that single optical fibre, being distinguished at the datalogger by wavelength division multiplexing (WDM) techniques.

3. MATERIALS

Direct tensile tests were conducted on a Glass Fibre Reinforced Polymer (GFRP) mesh (Figure 1) featuring an embedded Fibre Bragg Grating (FBG) sensor. Specifically, 50 cm long single wire specimens (Figure 2a) were extracted from a pre-cured FRP mesh composed of glass fibres and a thermosetting primer, with a surface mass density of 335 g/m² and a grid spacing of 50 mm × 50 mm. The mesh exhibits a balanced

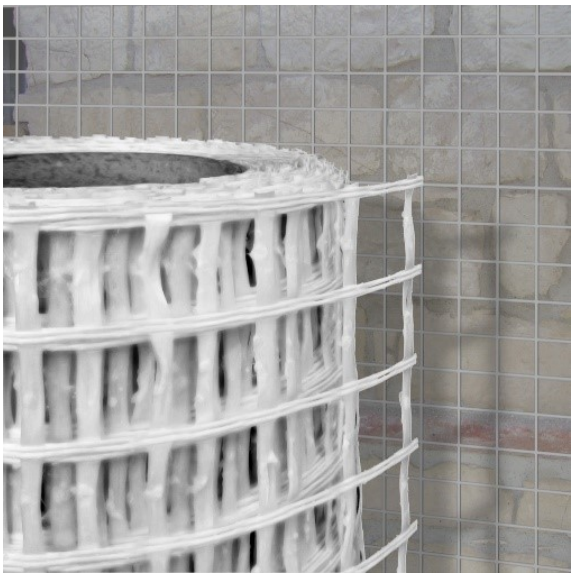

Figure 1. Glass Fibre Reinforced Polymer (GFRP) mesh.

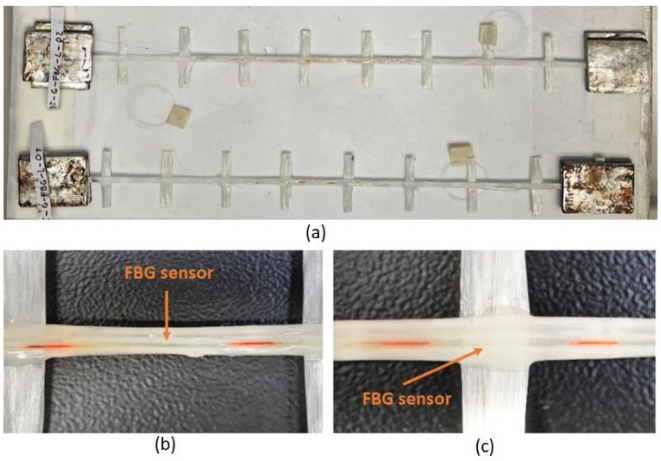

Figure 2. Single mesh wires with FBG sensors and ready to test (a), and detail of FBG in L (b) and X (c) locations.

structure, ensuring an equal amount of fibres in both the longitudinal (warp) and transversal (weft) directions, each with a design thickness of 0.044 mm. The cross-sectional area of a single GFRP mesh wire is 2.19 mm² [54]. It is noteworthy that glass, carbon, and aramid fibres are presently employed in the GFRP pre-cured meshes of Composite Reinforced Mortar (CRM) systems [55]. Glass fibres are preferred for their cost-effectiveness and their mechanical compatibility with masonry substrates, given their lower tensile modulus of elasticity compared to carbon and aramid. Additionally, GFRP mesh exhibits an inherent compatibility with optical fibre cables, also crafted from glass fibres.

FBG sensor produced on SMF28 optical fibres with acrylate coating were utilized. The length of the FBG sensor was 10 mm and it was provided with polyamide recoating. The standard production procedure of FBGs includes three steps: i) the stripping of the original coating at the grating location; ii) the modification of the refraction index to produce the diffraction grating; iii) the deposition of a new coating. Polyamide recoating, offered as premium commercial option, was preferred over the standard acrylate recoating, because of its superior structural features providing a better transfer of the deformation to the diffraction grating in the core of the optical fibre. The length of the FBG equal to 10 mm, given the size of the specimens, allowed considering the measurement as punctual. The sensor boasts a reflectivity exceeding 90 %, with a tolerance of +/- 0.15 nm on the central wavelength value, as per the datasheet [56].

In the preparation process, the mesh wires were cleansed with an alcoholic solution and left to dry. Subsequently, FBG sensors were glued using a bicomponent epoxy resin featuring a tensile strength of 30 N/mm² and a tensile modulus of elasticity of 1760 N/mm². The FBG sensors were strategically placed in the warp direction, either at midspan between two weft wires ("L" location, Figure 2b) or at the intersection between weft and warp ("X" location, Figure 2c). Specimens were labelled as DT-G-FBG-L or DT-G-FBG-X, where DT denotes Direct Tensile, G represents Glass FRP mesh, FBG indicates the presence of FBG sensors, and L or X denotes the position of the sensor.

Following a 7-day resin curing period, 3 mm thick aluminium tabs were glued to the specimen ends to ensure proper gripping in the clamping wedges of the testing machine, rendering the specimens ready for subsequent testing procedures (Figure 2a).

Figure 3. Fibre cutter (a) and splicer (b).

4. TEST SETUP AND EQUIPMENT

The tensile tests were conducted using an MTS Landmark Servohydraulic machine with a 100 kN load capacity, employing a displacement-controlled protocol at a stroke displacement rate of 2 mm/s. Load data were recorded by an integrated load cell at a sampling frequency of 10 Hz. Simultaneously, the reflected wavelength shift was recorded by an FS22 Industrial BraggMETER HBM optical interrogator at a sampling frequency of 1 Hz. Bragg-METER industrial interrogators are specifically designed to interrogate Bragg fibre grating sensors. Based on continuous laser scanning technology, these interrogators include a traceable wavelength reference that provides continuous calibration and ensures system accuracy in long-term operation. Before taking the measurement, it was necessary to weld the optical fibre housing the sensor to the optical fibre connector of the acquisition system. The external coating of the fibre was removed by manual stripping with scissors suitable for the operation and then the fibre was cut precisely using a special fibre cutter (Figure 3a) equipped with a diamond blade. This operation was necessary to obtain faces that were parallel to each other and thus guarantee minimum losses during welding. Once the fibre had been prepared, the two ends of the fibre and the connector were inserted into the splicer (Figure 3b), which automatically aligned and welded them by electrofusion.

To complement the mechanical measurements, Digital Image Correlation (DIC) strain analyses were performed using photos taken at 3 s intervals with a Nikon reflex camera. Two artificial markers, consisting of metal tabs with speckle patterns, were applied to the specimen. DIC allowed tracking their relative displacement, enabling continuous monitoring of the central portion of the specimen, which also included the embedded FBG sensor (Figure 4 and Figure 5). Stable light conditions were ensured by two LED spotlights. DIC analyses were conducted using the open-source Matlab-based NCorr software [57].

A minor pre-load was applied before initiating the tests to enhance alignment. The testing protocol included sets of unloading-reloading cycles, comprising 5 cycles each, between 0 ‰ and 1 ‰ axial strain, 0 ‰ and 2 ‰, and 0 ‰ and 5 ‰. The final phase involved a ramp from 0 ‰ to the failure point of the FBG sensor, providing a comprehensive characterization of the mechanical response of the integrated CRM-FBG specimen under varying strain conditions. Testing setup and protocol were developed based on scientific literature [58] and certification standards for inorganic matrix-based composites [59], [55].

5. TEST RESULTS

The initial characterization tests showed a linear elastic response of the mesh wires, persisting even during the unloading-reloading phases, ultimately leading to a purely brittle failure. The average tensile strength was determined as 1321 N/mm², with an ultimate strain of 1.50 % and a tensile modulus of elasticity of 100.8 kN/mm².

Figure 6 presents the comprehensive results of DIC and FBG measurements, with each subplot corresponding to a distinct specimen. DIC strain (ε_{DIC}) was computed as the relative displacement between two artificial markers divided by their initial distance. FBG strain (ε_{FBG}) was derived from the wavelength variation using Equation (2).

The Root Mean Square Deviation (RMSD) was employed to assess the error between FBG and DIC strain data (3):

Figure 4. Experimental setup (front view).

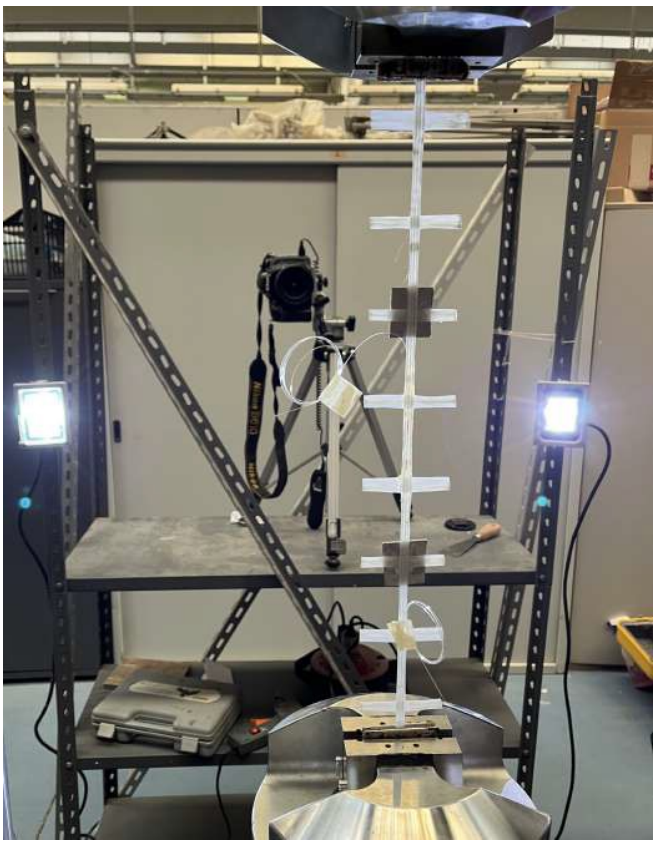

Figure 5. Experimental setup (rear view).

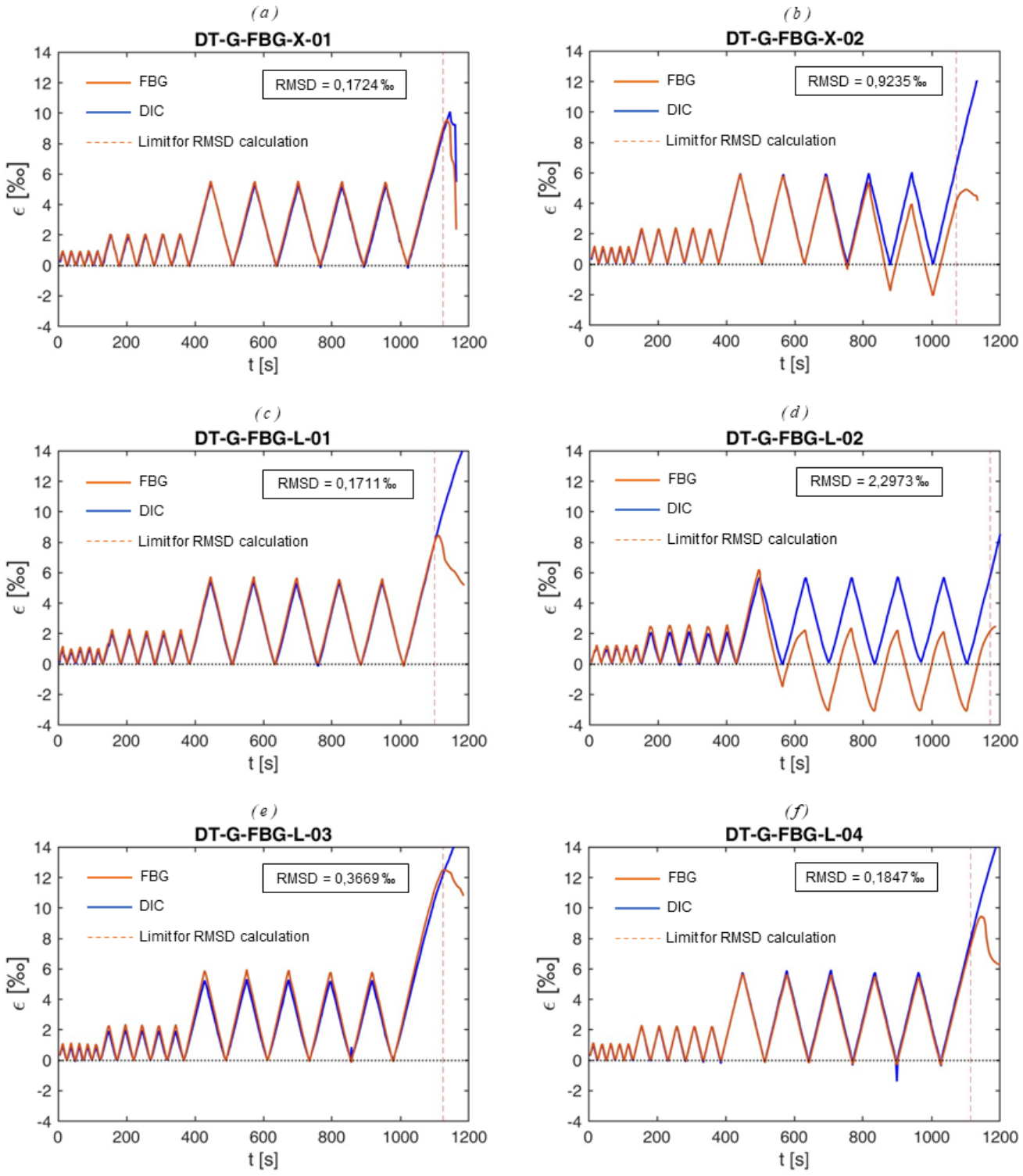

Figure 6. Response curves of direct tensile tests. FBG sensors were placed at the intersection between weft and warp (X location) in subplots a-b and at midspan between two weft wires (L location) in subplots c-f.

$$RMSD = \sqrt{\frac{\sum_{i=1}^{T}(\varepsilon_{\mathrm{DIC},i} - \varepsilon_{\mathrm{FBG},i})^2}{T}} \quad (3)$$

where i indicates the i-th time instant and T is the total of time instants considered for the calculation.

As a whole, the graphs of Figure 6 show excellent agreement between FBG and DIC strains in the initial test phases, and RMSD values ranged between 0.05 ‰ and 2.3 ‰. Then, at strain values between 5 ‰ and 12 ‰, slippage occurred in the FBG sensor, inducing a discrepancy between the two measurements, see, for instance, Figure 3 b) and d). This slippage was detectable during the test execution, and notably took place under strain values correspond to a $\Delta\lambda_B$ greater than 7 nm, representing the declared limit strain for the polyamide coating.

Detailed analysis of individual specimens revealed variations in performance. For instance, in the DT-G-FBG-X-01 specimen, no slippage occurred before rupture at 10 ‰, with an 0.172 ‰ RMSD value, while in DT-G-FBG-X-02, slippage initiated

during the third 5 ‰ cycle and completed at 8 ‰, with a 0.92 ‰ RMSD. In the DT-G-FBG-L-01 specimen, good overlap between measurements persisted until the final ramp, where slippage occurred at 8 ‰ strain. This specimen exhibited the minimum RMSD value of 0.171 ‰. In DT-G-FBG-L-02, the sensor functioned correctly until the first cycle at 5 ‰ and showed the largest RMSD value of 2.30 ‰, while DT-G-FBG-L-03 exhibited a peak in ε_{DIC} value at the end of the 4th cycle at 5 ‰ due to wire rotation, undetected by the FBG sensor. Slippage occurred at 12 ‰ in this case. Similar rotations were observed in DT-G-FBG-L-04, with slippage occurring at 10 ‰.

On average, the RMDS value resulted 0.686 ‰. In all the 6 specimens tested, FBG and DIC strain data agreed for all the load cycles at 1 ‰ and at 2 ‰ target strain. In 4 specimens out of 6, the FBG sensors worked properly also during the following cycles at 5 ‰ strain and during the final load phase, reading reliable elongation until an average strain level of 9.2 ‰. In the remaining 2 specimens, some mismatch appeared during the cycles at 5 ‰ strain. Clearly, more tests would be necessary for a complete statistical discussion of results, but the fundamental agreement of the experiments described above from a global functioning viewpoint indicates that FBGs can be considered as reliable strain sensors when bonded onto the GFRP mesh of CRM composites.

6. CONCLUSIONS

This study introduced a prototype integrated system of Composite Reinforced Mortar and optical Fibre Bragg Grating sensors (CRM-FBG), demonstrating its potential for upgrade and monitoring of existing structures, particularly in the realm of architectural heritage.

Direct tensile tests showcased the agreement between FBG sensor-derived strain data and Digital Image Correlation, even during unloading-reloading cycles and up to a strain of at least 5 ‰, which might be considered as indicative of structural damage. This suggests that FBG sensors hold promise for Structural Health Monitoring, because they can measure strain on the textile and thus detect a stress state change and a possible initiation of a failure mechanism. However, at higher strains, the occurrence of FBG sensor slippage or optical fibre rupture led to unreliable or unavailable measurements in some instances.

As far as the position of the sensor is concerned, there appeared to be no difference between the two tested positions. However, L-position made the FBG-CRM bonding phase more precise because the wire at this point is flat, whereas at the intersection of the mesh (X-position) the surface is curved.

The findings presented in this work need to be complemented by further experiments. First, the response of FBG sensors when embedded into the inorganic matrix of the CRM composite needs to be investigated by direct tensile tests on coupon specimens and by shear bond tests. The interaction of the instrumented GFRP mesh with the mortar, especially when cracks develop or mesh-to-mortar slippage activates, is expected to affect strain data. This would indicate that the goal of providing information on damage development is achieved, but the reliability of recorded strains and the length of the mesh that is effectively monitored (given the ununiform strain field associated with cracks) should be determined.

Furthermore, the durability of CRM-FBG system should be investigated, e. g., through laboratory tests after artificial accelerated aging, to complement its characterization for long-term applications, which is crucial for the lasting protection of retrofitted/monitored structures.

Finally, with a view to the use of the proposed CRM-FBG technology for SHM applications in engineering practice (which is beyond the scope of this paper), other issues need to be tackled to optimize system architecture. Specific structural features and expected locations of significant damage will orient the strengthening/monitoring design to install sensors where (and only where) necessary, pursuing a feasible balance with costs, installation/cabling efforts, and storage, transfer, post-processing, and analysis of recorded data.

ACKNOWLEDGEMENTS

This project forms a component of Giovanni Moretti's doctoral research, supported by Regione Lazio (G03269/2022) and cofunded by Indagini Strutturali Srl (Rome, Italy). Gratitude is extended to Kimia SpA (Perugia, Italy) for their provision of strengthening materials and to Engineer Stefano Agnetti for his valuable technical guidance. This work was carried out within the Research Project "Cultural Heritage Active Innovation for next-gen sustainable society (CHANGES)" funded by the National Recovery and Resilience Plan (NRRP), Mission 4, Component 2, Investment 1.3 supported by the "Next Generation EU" Programme of the European Union.

REFERENCES

[1] N. Gattesco, L. Boem, A. Dudine, Diagonal compression tests on masonry walls strengthened with a GFRP mesh reinforced mortar coatin, Bull Earthquake Eng 13 (2015), pp. 1703-1726. DOI: 10.1007/s10518-014-9684-z

[2] S. De Santis, G. De Felice, Shake table tests on a tuff masonry structure strengthened with composite reinforced mortar, Composite Structures 275 (2021), 114508. DOI: 10.1016/j.compstruct.2021.114508

[3] S. De Santis, F. Roscini, G. De Felice, Retrofitting of masonry vaults by basalt-textile reinforced mortar overlays, International Journal of Architectural Heritage 13 (2019) 7, pp. 1061-1077. DOI: 10.1080/15583058.2019.1597947

[4] S. Babaeidarabad, F. De Caso, A. Nanni, Out-of-Plane Behavior of URM Walls Strengthened with Fabric-Reinforced Cementitious Matrix Composite, J. Compos. Constr. 18 (2013), 04013057. DOI: 10.1061/(ASCE)CC.1943-5614.0000457

[5] S. De Santis, G. De Canio, G. De Felice, P. Meriggi, I. Roselli, Out-of-plane seismic retrofitting of masonry walls with Textile Reinforced Mortar composites, Bulletin of Earthquake Engineering 17 (2019) 11, pp. 6265–6300. DOI: 10.1007/s10518-019-00701-5

[6] A. Dalalbashi, S. De Santis, B. Ghiassi, D.V. Oliveira, Slip rate effects and cyclic behaviour of textile-to-matrix bond in textile reinforced mortar composites, Materials and Structures 54 (2021), 108. DOI: 10.1617/s11527-021-01706-w

[7] S. Fares, R. Fugger, S. De Santis, G. de Felice, Strength, bond and durability of stainless steel reinforced grout, Construction and Building Materials 322 (2022), 126465. DOI: 10.1016/j.conbuildmat.2022.126465

[8] G.E. Thermou, S. De Santis, G. de Felice, S. Alotaibi, R. Roscini, I. Hajirasouliha, M. Guadagnini, Bond Behaviour of Multi-Ply Steel Reinforced Grout Composites, Construction and Building Materials 305 (2021), 124750. DOI: 10.1016/j.conbuildmat.2021.124750

[9] P. Meriggi, F. Nerilli, S. Fares, R. Fugger, S. Marfia, E. Sacco, G. De Felice, Shear Mechanisms in Fabric-Reinforced Cementitious Matrix Overlays: Experimental and Numerical Investigation, Journal of Composites for Construction 27 (2023) 04023032.

DOI: 10.1061/JCCOF2.CCENG-4115
[10] P. Meriggi, S. De Santis, S. Fares, G. de Felice, Design of the shear strengthening of masonry walls with fabric reinforced cementitious matrix, Construction and Building Materials 279 (2021), 122452.
DOI: 10.1016/j.conbuildmat.2021.122452
[11] P. Meriggi, G. de Felice, S. De Santis, Design of the out-of-plane strengthening of masonry walls with fabric reinforced cementitious matrix composites, Construction and Building Materials 240 (2020), 117946.
DOI: 10.1016/j.conbuildmat.2019.117946
[12] CNR-DT 215/2018: Guide for the design and construction of Externally Bonded Fibre Reinforced Inorganic Matrix systems for strengthening existing structures.
[13] ACI 549.6R-20: Guide to Design and Construction of Externally Bonded Fabric-Reinforced Cementitious Matrix (FRCM) and Steel-Reinforced Grout (SRG) Systems for Repair and Strengthening Masonry Structures.
[14] P. Meriggi, G. de Felice, S. de Santis, M. Morganti, F. Roscini, Durability of steel reinforced grout systems subjected to freezing-and-thawing conditioning, Proceedings of the 1st fib Italy YMG Symposium on Concrete and Concrete Structures, FIBPRO 2019, Parma, Italy, 15 October 2019, pp. 47–55.
[15] CSLLPP, Linee Guida per la identificazione, la qualificazione ed il controllo di accettazione di compositi fibrorinforzati a matrice inorganica (FRCM) da utilizzarsi per il consolidamento strutturali di costruzioni esistenti, 2018. [In Italian]
[16] EAD 340392-00-0104, CRM (Composite Reinforced Mortar) Systems for strengthening concrete and masonry structures, 2018.
[17] F. Ceroni, A. Bonati, V. Galimberti, A. Occhiuzzi, Effects of environmental conditioning on the bond behavior of FRP and FRCM systems applied to concrete elements, J. Eng. Mech. 144 (2018) 04017144, pp. 1-15.
DOI: 10.1061/(ASCE)EM.1943-7889.0001375
[18] M. De Munck, M. El Kadi, E. Tsangouri, J. Vervloet, S. Verbruggen, J. Wastiels, T. Tysmans, O. Remy, Influence of environmental loading on the tensile and cracking behaviour of textile reinforced cementitious composites, Constr. Build. Mater. 181 (2019), pp. 325-334.
DOI: 10.1016/j.conbuildmat.2018.06.045
[19] F. Micelli, M.A. Aiello, Residual tensile strength of dry and impregnated reinforcement fibres after exposure to alkaline environments, Composites Part B: Engineering 159 (2019), pp. 490-501.
DOI: 10.1016/j.compositesb.2017.03.005
[20] J. Donnini, Durability of glass FRCM systems: Effects of different environments on mechanical properties, Compos. Part B Eng. 174 (2019), 107047.
DOI: 10.1016/j.compositesb.2019.107047
[21] F. Micelli, A. Franco, R. Greppi, M.A. Aiello, Durability of CRM reinforcements, Life-Cycle of Structures and Infrastructure Systems – Proc. of the 8th International Symposium on Life-Cycle Civil Engineering, IALCCE 2023, Milan, Italy, 2 – 6 July 2023, pp. 2820-2827.
DOI: 10.1201/9781003323020-343
[22] E. Bertolesi, M. Fagone, T. Rotunno, E. Grande, G. Milani, Experimental characterization of the textile-to-mortar bond through distributed optical sensors, Construction and Building Materials, 326 (2022), 126640.
DOI: 10.1016/j.conbuildmat.2022.126640
[23] CNR. CNR-DT 200 R1/2013. Istruzioni per la Progettazione, l'Esecuzione ed il Controllo di Interventi di Consolidamento Statico mediante l'utilizzo di Compositi Fibrorinforzati. [In Italian]
[24] CNR. CNR-DT 215 2018. Istruzioni per la Progettazione, l'Esecuzione ed il Controllo di Interventi di Consolidamento Statico mediante l'utilizzo di Compositi Fibrorinforzati a Matrice Inorganica. [In Italian]
[25] K. Bremer, M. Wollweber, F. Weigand, M. Rahlves, M. Kuhne, R. Helbig, B. Roth, Fibre optic sensors for the structural health monitoring of building structures, Procedia Technology 26 (2016), pp. 524-529.
DOI: 10.1016/j.protcy.2016.08.065
[26] I. Roselli, A. Tatì, V. Fioriti, I. Bellagamba, M. Mongelli, R. Romano, G. De Canio, M. Barbera, M.M. Cianetti, Integrated approach to structural diagnosis by non-destructive techniques: the case of the Temple of Minerva Medica, Acta IMEKO 7 (2018) 3, pp. 13-19.
DOI: 10.21014/acta_imeko.v7i3.558
[27] L. Martins, Á. Ribeiro, M. d. C. Almeida, J. A. Sousa, Bringing optical metrology to testing and inspection activities in civil engineering, Acta IMEKO 10 (2021) 3, pp. 108-116.
DOI: 10.21014/acta_imeko.v10i3.1059
[28] A. D. Kersey, M. A. Davis, H. J. Patrick, M. LeBlanc, K. P. Koo, C. G. Askins, M. A. Putnam, E. J. Friebele, Fiber grating sensors, J. of Lightwave Technology 15 (1997) 8, pp. 1442-1463.
DOI: 10.1109/50.618377
[29] W. Liu, Y. Guo, L. Xiong, Y. Kuang, Fiber Bragg grating based displacement sensors: state of the art and trends, Sensor Review, 39 (2019), pp. 87-98.
DOI: 10.1108/SR-06-2017-0116
[30] J. Chen, B. Liu, H. Zhanh, Review of fiber Bragg grating sensor technology, Frontiers of optoelectronics in China, 4 (2011) 2, pp. 204-212.
DOI: 10.1007/s12200-011-0130-4
[31] X. Qiao, Z. Shao, W. Bao, Q. Rong, Fiber Bragg Grating Sensors for the Oil Industry, Sensors, 17 (2017) 429.
DOI: 10.3390/s17030429
[32] C.-Y. Hong, Y.-F. Zhang, M.-X. Zhang, L. M. G. Leung, L.-Q. Liu, Application of FBG sensors for geotechnical health monitoring, a review of sensor design, implementation methods and packaging techniques, Sensors and Actuators A, 244 (2016), pp. 184-197.
DOI: 10.1016/j.sna.2016.04.033
[33] J. Lai, J. Qiu, H. Fan, Q. Zhang, Z. Hu, J. Wang, J. Chen, Fiber Bragg Grating Sensors-Based In Situ Monitoring and Safety Assessment of Loess Tunnel, Journal of Sensors, 2016 (2016), 8658290.
DOI: 10.1155/2016/8658290
[34] L. Ren, Z.-g. Jia, H.-N. Li e G. Song, Design and experimental study on FBG hoop-strain sensor in pipeline monitoring, Optical Fiber Technology, 20 (2014), pp. 15-23.
DOI: 10.1016/j.yofte.2013.11.004
[35] B. Glisic, 17 - Fiber optic sensors for subsea structural health monitoring, in: Subsea Optics and Imaging. J. Watson, O. Zielinski (editors). Woodhead Publishing, 2013, ISBN 9780857093417, pp. 434-470.
[36] A. Quattrocchi, R. Montanini, Development and verification of self-sensing structures printed in additive manufacturing: a preliminary study, Acta IMEKO 12 (2023) 2, pp. 1-7.
DOI: 10.21014/actaimeko.v12i2.1431
[37] R. Scott, P. Banerji, S. Chikermane, S. Srinivasan, M. Basheer, Commissioning and Evaluation of a Fiber-Optic Sensor System for Bridge Monitoring, IEEE Sensors Journal, 13 (2013) 6508853, pp. 2555-2562.
DOI: 10.1109/JSEN.2013.2256599
[38] K. Yüksel, D. Kinet, V. Moeyaert, G. Kouroussis, C. Caucheteur, Railway monitoring system using optical fiber grating accelerometers, Smart Materials and Structures, 27 (2018) 105033.
DOI: 10.1088/1361-665X/aadb62
[39] E. Verstrynge, K. De Wilder, A. Drougkas, E. Voet, K. Van Balen, M. Wevers, Crack monitoring in historical masonry with distributed strain and acoustic emission sensing techniques, Construction and Building Materials, 162 (2018), pp. 898-907.
DOI: 10.1016/j.conbuildmat.2018.01.103
[40] P. Antunes, H. Lima, H. Varum, P. André, Optical fiber sensors for static and dynamic health monitoring of civil engineering infrastructures: Abode wall case study, Measurement, 45 (2012), pp. 1695-1705.
DOI: 10.1016/j.measurement.2012.04.018

[41] W. Chung, D. Kang, Full-scale test of a concrete box girder using FBG sensing system, Engineering Structures 30 (2008) 3, pp. 643-652.
DOI: 10.1016/j.engstruct.2007.05.003

[42] A. P. Adewuyi, Z. Wu, N. H. M. Kammrujaman Serker, Assessment of vibration-based damage identification methods using displacement and distributed strain measurements, Structural Health Monitoring 8 (2009) 6, pp. 443-461.
DOI: 10.1177/1475921709340964

[43] D. Zangani, C. Fuggini, G. Loriga, Electronic textiles for geotechnical and civil engineering, in: Electronic Textiles: Smart Fabrics and Wearable Technology. T. Dias (Editor). Woodhead Publishing, 2015, ISBN 978-008100223-0, 978-008100201-8, pp. 275 - 300.

[44] S. Liehr, P. Lenke, K. Krebber, M. Seeger, E. Thiele, H. Metschies, B. Gebreselassie, J. C. Münich, L. Stempniewski, Distributed strain measurement with polymer optical fibers integrated into multifunctional geotextiles, Proc. of SPIE - The International Society for Optical Engineering, Optical Sensors, Strasbourg, France, 7-10 April 2008, vol. 7003, no. 700302.
DOI: 10.1117/12.780508

[45] D. Zangani, POLYTECT-Polyfunctional Technical Textiles against Natural Hazards—Project No. NMP2-CT-2006-026789, 2010. Online [Accessed 23 January 2024]
https://cordis.europa.eu/project/id/26789/reporting

[46] F. Valvona, J. Toti, V. Gattulli, F. Potenza, Effective seismic strengthening and monitoring of a masonry vault by using Glass Fiber Reinforced Cementitious Matrix with embedded Fiber Bragg Grating sensors, Composites Part B, 113 (2017), pp. 355-370.
DOI: 10.1016/j.compositesb.2017.01.024

[47] A. Shaikh, L. J. Butler, Self-sensing fabric reinforced cementitious matrix systems for combined strengthening and monitoring of concrete structures, Construction and Building Materials, 331 (2022), 127243.
DOI: 10.1016/j.conbuildmat.2022.127243

[48] A. Coricciati, I. Ingrosso, A. Sergi, A. Largo, Application of Smart FRP Devices for the Structural Health Monitoring of heritage buildings - A case study: The monastery of Sant'Angelo d'Ocre, Key Engineering Materials, 747 (2017), pp. 448-455.
DOI: 10.4028/www.scientific.net/kem.747.448

[49] Z. C. Tetta, Shear Strengthening of Concrete Members with Textile Reinforced Mortar (TRM), Ph.D. Thesis, University of Nottingham, Nottingham, UK, 2017. Online [Accessed 16 February 2024]
https://eprints.nottingham.ac.uk/43314/

[50] M. Saidi, A. Gabor, Experimental analysis of the tensile behaviour of textile reinforced cementitious matrix composites using distributed fibre optic sensing (DFOS) technology, Construction and Building Materials, 230 (2020), 117027.
DOI: 10.1016/j.conbuildmat.2019.117027

[51] L. Stempniewski, POLYMAST Polyfunctional Technical Textiles for the Protection and Monitoring of Masonry Structures against Earthquake, in: Transnational Access within the SERIES Project: SEVENTH FRAMEWORK PROGRAM Capacities Specific Programme Research Infrastructures - Project No.227887, Final Report, May 2011.

[52] H. Lima, R. Ribeiro, R. Nogueira, L. Silva, I. Abe, J. L. Pinto, Continuous monitoring of setting and hardening of mortar using FBG sensors, Proc. of SPIE – The International Society for Optical Engineering, Optical Sensing Technology and Applications, Prague, Czech Republic, 16-18 April 2007, vol. 6585, article id. 65850D.
DOI: 10.1117/12.722483

[53] H. Pei, B. Zhang, Z. Li, H. Ma, J. Zhang, Measurement of early-age strains in mortar specimens subjected to cyclic temperature, Materials Letters 142 (2015), pp. 150-152.
DOI: 10.1016/j.matlet.2014.11.071

[54] Kimia, Kimitech WALLMESH MR Technical data sheet. Online [Accessed 23 April 2024]
https://www.kimia.it/sites/default/files/docs/st/en-kimitech-wallmesh-mr.pdf

[55] CSLLPP, Linea Guida per la identificazione, la qualificazione ed il controllo di accettazione dei sistemi a rete preformata in materiali compositi fibrorinforzati a matrice polimerica da utilizzarsi per il consolidamento strutturale di costruzioni esistenti con la tecnica dell'intonaco armato CRM (Composite Reinforced Mortar), 2019. [In Italian]

[56] Broptics Technology Inc., Broptics OS 1500 Technical data sheet. Online [Accessed 23 April 2024]
http://www.broptics.com/products_sensor.htm

[57] J. Blaber, B. Adair, A. Antoniou, Ncorr: Open-Source 2D Digital Image Correlation Matlab Software, Experimental Mechanics, 55 (2015), pp. 1105-1122.
DOI: 10.1007/s11340-015-0009-1

[58] S. De Santis, F.G. Carozzi, G. de Felice, C. Poggi, Test methods for Textile Reinforced Mortar systems, Composites Part B: Engineering 127 (2017), pp. 121-132.
DOI: 10.1016/j.compositesb.2017.03.016

[59] CSLLPP, Linea Guida per la identificazione, la qualificazione ed il controllo di accettazione di compositi fibrorinforzati a matrice inorganica (FRCM) da utilizzarsi per il consolidamento strutturale di costruzioni esistenti, 2018. [In Italian]